UDC621.391

MULTI-SENSOR FUSION FOR MOBILE ROBOT PERCEPTION

Bin Zhang, student gr.363411

Belarusian State University of Informatics and Radioelectronics1, Minsk, Republic of Belarus

Jun Ma – Assistant

Annotation. This paper presents a multi-sensor fusion perception system to overcome key limitations of single-line LiDAR in mobile robots, including pose drift, vertical blind zones, and poor robustness against transparent surfaces or sensor failures. The proposed architecture integrates LiDAR-IMU tightly-coupled odometry, RGB-D camera-based 3D mapping using ORB-SLAM2, and ultrasonic near-field detection. The design is expected to improve positioning accuracy and environmental awareness in indoor scenarios. The work is currently at the design phase, with physical implementation planned for future research.

Keywords. 2D LiDAR, Raspberry Pi, Obstacle Avoidance, Indoor Mobile Robot, LiDAR SLAM.

Introduction

With the rapid development of AI and sensor technologies, mobile robots have expanded from industrial automation to healthcare, logistics, and domestic service [1]. LiDAR has become a core navigation sensor due to its high accuracy and fast response [2]. Within ROS2 [3], low-cost mobile robot development has become a research hotspot. Single-line LiDAR offers high accuracy, good real-time performance, and low cost. However, relying solely on it for both obstacle avoidance and mapping presents several limitations. First, it only obtains 2D planar information, missing low-height or suspended obstacles, and has a near-field blind zone. Second, pure LiDAR odometry lacks motion priors, making it prone to pose drift during rapid motion. Third, it has blind zones for glass and mirrors, struggles with dynamic objects, and suffers from single points of failure. To validate these limitations, a distributed control platform with upper and lower computers was constructed. The upper computer (Raspberry Pi 4B, ROS2 Humble) handles LiDAR data, obstacle avoidance, and visualization. The lower computer (Arduino Uno) receives speed commands, performs inverse kinematics for Mecanum wheels, and controls four DC motors via an L293D driver module. Figure 1 shows the system hardware architecture.

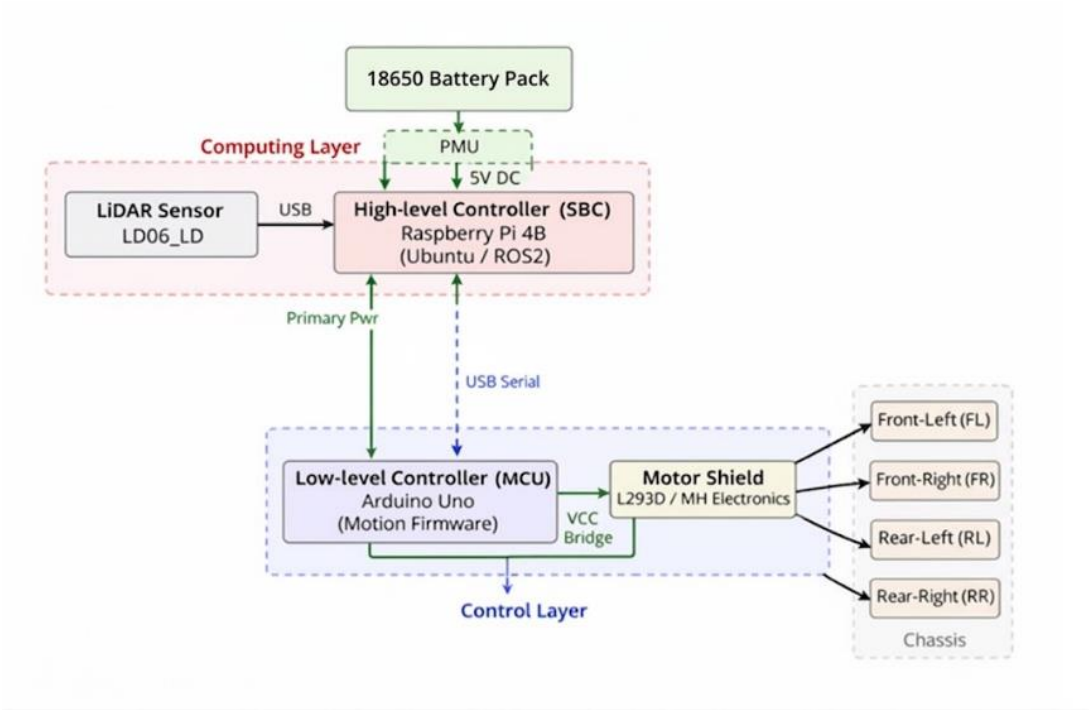

Figure 1 – System hardware architecture diagram

In preliminary SLAM mapping and obstacle avoidance experiments, three theoretical issues were validated. First, mapping drift caused by motion estimation degradation. Without IMU or high-precision encoders, pure LiDAR odometry exhibited significant mapping drift during rapid rotation and movement, manifested as point cloud ghosting and pose offset. Figure 2 shows the mapping drift in pure LiDAR SLAM without loop closure. Second, obstacle missed detection caused by spatial perception limitations. The LD06 2D LiDAR is mounted on the robot's roof (approximately 10 cm above ground) and can only acquire horizontal plane scan data. When obstacle height is below the LiDAR scan plane, the system fails to detect it

entirely. Third, lack of environmental adaptability and system robustness. When approaching glass windows or mirrored furniture, severe missing occurs in the LiDAR point cloud over large reflective surfaces. When the sensor experiences temporary disconnection, the robot immediately falls into a "perception failure" state. Addressing these three problems, this paper proposes corresponding solutions: introducing an RGB-D camera to obtain obstacle height information, fusing IMU with LiDAR to construct tightly-coupled odometry, and adding fault detection and degraded operation mechanisms.

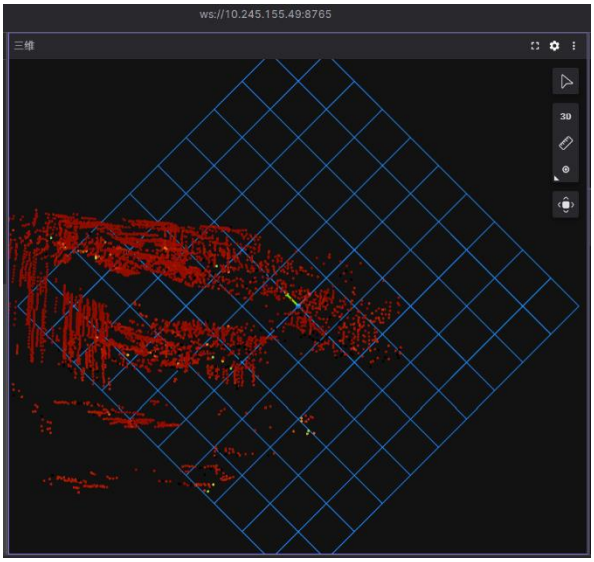

Figure 2 – Mapping drift in pure LiDAR SLAM without loop closure

Suppression of Motion Estimation Degradation: LiDAR-IMU Fusion Odometry

To address pose drift during rapid rotation, in feature-sparse environments, and on rough terrain, this paper proposes integrating an IMU with LiDAR to construct tightly-coupled LiDAR-IMU odometry. An MPU6050 six-axis IMU is selected with an output frequency of 200 Hz. Time alignment with LiDAR is achieved using ROS2's joint time synchronization mechanism. The fusion algorithm adopts a tightly-coupled framework based on an Error State Kalman Filter (ESKF) [4]. IMU data provides high-frequency state propagation for pose prediction between two LiDAR scans. Upon arrival of a new LiDAR scan, feature points are extracted and scan-matched against the local map to obtain observation residuals. The filter update corrects accumulated IMU error and estimates IMU biases online. In feature-sparse environments, the system adaptively increases IMU prediction weight to avoid pose mutation caused by scan matching failure [4]. To address vehicle pitch angle changes on rough terrain, attitude angles estimated by the IMU are fed back to the LiDAR point cloud preprocessing module. The raw point cloud is rotationally corrected before scan matching, effectively suppressing mapping distortion caused by vehicle tilt. This fusion odometry provides stable pose estimation for the entire system, supporting subsequent mapping and obstacle avoidance functions.

Enhancement of System Robustness: 3D Environmental Perception Based on an RGB-D Camera

Building upon stable pose estimation from LiDAR-IMU fusion odometry, this paper introduces an RGB-D camera to address the vertical perception blind zone problem. The LD06 LiDAR can only acquire two-dimensional horizontal information, failing to detect low-height or suspended obstacles and unable to identify obstacle categories. The system defaults to using the RGB-D camera as the core mapping sensor, running an ORB-SLAM2 [5] visual-inertial tightly-coupled SLAM system. In environments with good lighting and rich texture, it constructs a 3D point cloud map containing obstacle height information and, combined with lightweight object detection algorithms, identifies obstacle types that LiDAR cannot perceive. Due to Raspberry Pi computational limitations, the system does not support simultaneous operation of LiDAR and RGB-D camera. Consequently, a manual switching mode is adopted in practical deployment. By default, the RGB-D camera is responsible for mapping and object recognition. When the robot enters scenes with insufficient lighting, texture scarcity, or excessive dynamic objects, the user can manually shut down ORB-SLAM2 and switch to LiDAR SLAM mode. Regarding obstacle avoidance functionality, regardless of which sensor is currently used for mapping, LiDAR always remains active as the primary obstacle avoidance sensor. Leveraging its high ranging accuracy and fast response speed, LiDAR ensures real-time obstacle avoidance performance in most scenarios. Simultaneously, the position information of low-height and suspended obstacles identified by the RGB-D camera is synchronized to the obstacle avoidance module. This design achieves a balance between perception completeness and operational safety under limited computational resources.

Enhancement of System Robustness: Near-Field Obstacle Avoidance Using Ultrasonic Sensors

2D LiDAR has inherent limitations: its scanning plane is fixed, rendering it ineffective against transparent or reflective materials like glass and mirrors, and it possesses a near-field blind zone. Mounted approximately 10 cm above ground, areas above and below its scanning plane are entirely outside its detection range. To compensate for these defects, this section introduces ultrasonic sensors as supplementary obstacle avoidance. Two to three HC-SR04 ultrasonic sensors are installed on the front of the robot chassis to provide gapless scanning of the area directly in front of the robot, focusing on detecting low-height obstacles below the LiDAR's scanning plane. Ultrasonic sensors are insensitive to transparent and reflective materials, effectively detecting obstacles that LiDAR struggles with. In the obstacle avoidance logic, LiDAR holds first priority with a safety threshold of 30 cm. Ultrasonic sensors act as a second defense with a more conservative safety threshold of 15 cm. When LiDAR fails to trigger avoidance due to special materials, blind zones, or height limitations, and an ultrasonic sensor detects an obstacle within 15 cm, the system immediately executes deceleration and backward turning to re-plan the path. The RGB-D camera handles predictive avoidance of pre-identified dangerous areas, complementing the real-time detection capability of the ultrasonic sensors.

Conclusion

This chapter addresses inherent limitations of single-line LiDAR by introducing an IMU, an RGB-D camera, and ultrasonic sensors, thereby constructing a multi-sensor fusion perception and localization system. The LiDAR-IMU fusion odometry mitigates pose drift. The RGB-D camera serves as the default mapping sensor, building 3D point cloud maps to solve the vertical perception blind zone problem. Ultrasonic sensors act as supplementary obstacle avoidance tools, filling gaps related to transparent materials and the near-field blind zone. Table 1 summarizes the roles of different sensors.

Table 1 – Roles of Different Sensors

Sensor	Normal Operating Environment	Advantages	Limitations	Role
LiDAR	All lighting conditions, most indoor scenes	High ranging accuracy, fast response, unaffected by light, independent of SLAM operation	The scanning plane is fixed, which may fails to work on transparent or reflective materials and creates a blind spot near the vehicle body	Primary obstacle avoidance sensor (always on); horizontal plane obstacle detection; performs SLAM mapping when RGB-D camera is unavailable
RGB-D Camera	Good lighting, rich texture, scenes with few dynamic objects	3D mapping, identification of low/suspended obstacles and identification of ground height changes in the road surface	Fails in low/excessive light, texture scarcity, or many dynamic objects; high computational cost	Primary mapping sensor (default mode); responsible for 3D map construction and obstacle recognition
Ultrasonic	All lighting conditions, short-range detection	Effective for transparent/reflective materials, fills frontal blind zone of LiDAR, fast response, low computational cost	Cannot detect ground height changes, limited detection range, low accuracy	Supplementary obstacle avoidance for LiDAR (second priority); provides degraded-mode safety during sensor failure

References:

1.Islamgozhayev T., Kalimoldayev M., Eleusinov A., Mazhitov S., Mamyrbayev O. // Open Eng. 2016. Vol. 6. P. 347–352.
2. Zhao Y., Li Y., Shang Y., et al. // Telemetry & Telecontrol. 2014. No. 5. P. 4–22.
3. Macenski S., Foote T., Gerkey B., Lalancette C., Woodall W. // Science Robotics. 2022. Vol. 7. P. eabm6074.
4. Xu W., Zhang F. // IEEE Robotics and Automation Letters. 2021. Vol. 6. P. 3317–3324.
5. Mur-Artal R., Tardós J. D. // IEEE Transactions on Robotics. 2017. Vol. 33. P. 1255–1262.